

NEW Fe(III), Co(II), Ni(II), Cu(II), AND Zn(II) MIXED-LIGAND COMPLEXES: STRUCTURAL, DFT, BIOLOGICAL, AND MOLECULAR DOCKING STUDIES

Hany M. Abd El-Lateef^{1,2*}, Ali M. Ali², Mai M. Khalaf^{1,2} and Aly Abdou²

¹Department of Chemistry, College of Science, King Faisal University, Al-Ahsa 31982, Saudi Arabia

²Department of Chemistry, Faculty of Science, Sohag University, Sohag 82534, Egypt

(Received November 21, 2023; Revised December 12, 2023; Accepted December 18, 2023)

ABSTRACT. The primary objective of the current framework was to synthesize novel mononuclear 1:1:1 complexes involving FeLG, CoLG, NiLG, CuLG, and ZnLG, where the ligand (L) is identified as 4-[(4-oxo-4,5-dihydro-1,3-thiazol-2-yl)hydrazono]methylphenyl-4-methylbenzenesulfonate, and glycine (G) serves as the ligand. Comprehensive characterization of the investigated complexes was achieved through various analytical techniques, including FTIR, UV-Vis spectroscopy, elemental analysis, mass spectra, magnetic susceptibility measurements, molar conductivity assessments, and thermogravimetric analysis (TGA). The determination of stoichiometry was performed employing the molar ratio technique, revealing the octahedral geometry inherent in the isolated metal complexes. Employing a density functional theory (DFT) approach, the molecular structures of the designated compounds were theoretically elevated, and quantum chemical descriptors were derived to provide a deeper insight into their electronic properties. Furthermore, the inhibitory potential of these compounds against fungal strains and pathogenic bacteria prevalent in the Arab environment was evaluated using the disc diffusion method, emphasizing their role in combating diseases affecting humans, animals, and plants. Notably, the metal complexes exhibited superior antibacterial activity, as evidenced by a higher activity index. Molecular docking investigations were conducted to ascertain the inhibitory effects of the compounds on the 1FJ4 protein, with ZnLG emerging as the compound with the highest binding affinity. These results suggest the promising candidacy of these compounds as antimicrobial agents, particularly in the context of combating bacterial and fungal infections.

KEY WORDS: Complexes, Antimicrobial, DFT, Schiff base, Molecular docking

INTRODUCTION

The fundamental reason for now restrictive the application of antibiotics in treating microbial illnesses is the advent of drug-resistant microbial pathogens [1, 2]. Complexes of Schiff-base have become increasingly significant in medicine as potential substitutes for conventional antibiotics [3, 4]. They gained a lot of significance because of the wide range of biological, analytical, and industrial implementations [5, 6], they have as well as their substantial function in organic synthesis and catalysis [7, 8]. In recent years, the numerous groups of biologically active coordination molecules have given a lot of attention to mixed transition metal complexes, with interest growing as a result of their adaptability and wide range of biological applications, such as in the treatment of cancer and antiviral, antimicrobial, and fungicidal components [9, 10].

Mixed ligand complexes are different from normal complexes and are more likely to have various biological characteristics [11] since they contain at least two diverse kinds of ligands with similar metal ions [12].

Recently, complexes based on amino acids have gained attention as an auspicious class of bioactive substances with wide potential for use as therapeutic medicines, diagnostic tools, and pathological examinations [13]. The twenty naturally occurring amino acids that makeup proteins, a chemical species that performs numerous biological tasks [14]. Numerous biological functions,

*Corresponding author. E-mail: hmahmed@kfu.edu.sa; hany_shubra@science.sohag.edu.eg (Hany M. Abd El-Lateef.); aly_abdou@science.sohag.edu.eg (Aly Abdou)

This work is licensed under the Creative Commons Attribution 4.0 International License

including oxygen transport, electron transfer, and oxidation, are carried out by complexes of transition metals that incorporate amino acids in peptides and proteins.

The addition of an amino-acid as a co-ligand may alter the coordination geometry, hydrophobicity, and planarity of produced complexes [15]. Additionally, mixed-ligand complexes are crucial components of metalloenzymes' catalytic centers. As a result, metalloenzyme models can be created by studying the interactions of amino acids and their mixed-ligand complexes with different transition metals.

Since Schiff-base complexes are novel materials with advantageous traits that can improve their biological function inside cells, their production and properties have drawn a lot of interest. Chemotherapy makes extensive use of such systems. In light of the above mentioned information, an effort has been completed to create novel complexes based on mixed ligands with favorable biological characteristics. Subsequently, a new series of metal: ligand: co-ligand (1:1:1) complexes will be produced and characterized. Both the new drugs' *in vitro* antibacterial efficacy and their molecular docking valuation against the 1FJ4 protein will be evaluated. Additionally, molecular and electronic structure DFT examination was researched.

EXPERIMENTAL

Chemicals and solvents

All of the chemicals employed in this study were of the highest purity possible and were of analytical reagent grade (AR). Ethyl bromoacetate, Fe(III) chloride, Ni(II) chloride, Co(II) chloride, Zn(II) chloride, Cu(II) chloride, and glycine were among the compounds used. Organic solvents such as acetonitrile, ethanol, and dimethylformamide (DMF) were spectroscopically free from BDH.

Synthesis

HL-ligand preparation

The target metal complexes were synthesized according to the previously reported method with slight modification [2, 16]: the starting ligand was simply prepared *via* the treatment of compound 4-[(carbamothioylhydrazono) methyl] phenyl 4-methylbenzenesulfonate with ethyl bromoacetate to give the corresponding ethyl 4-[(4-oxo-4,5-dihydro-1,3-thiazol-2-yl)hydrazono] methyl} phenyl 4-methylbenzenesulfonate, Scheme 1.

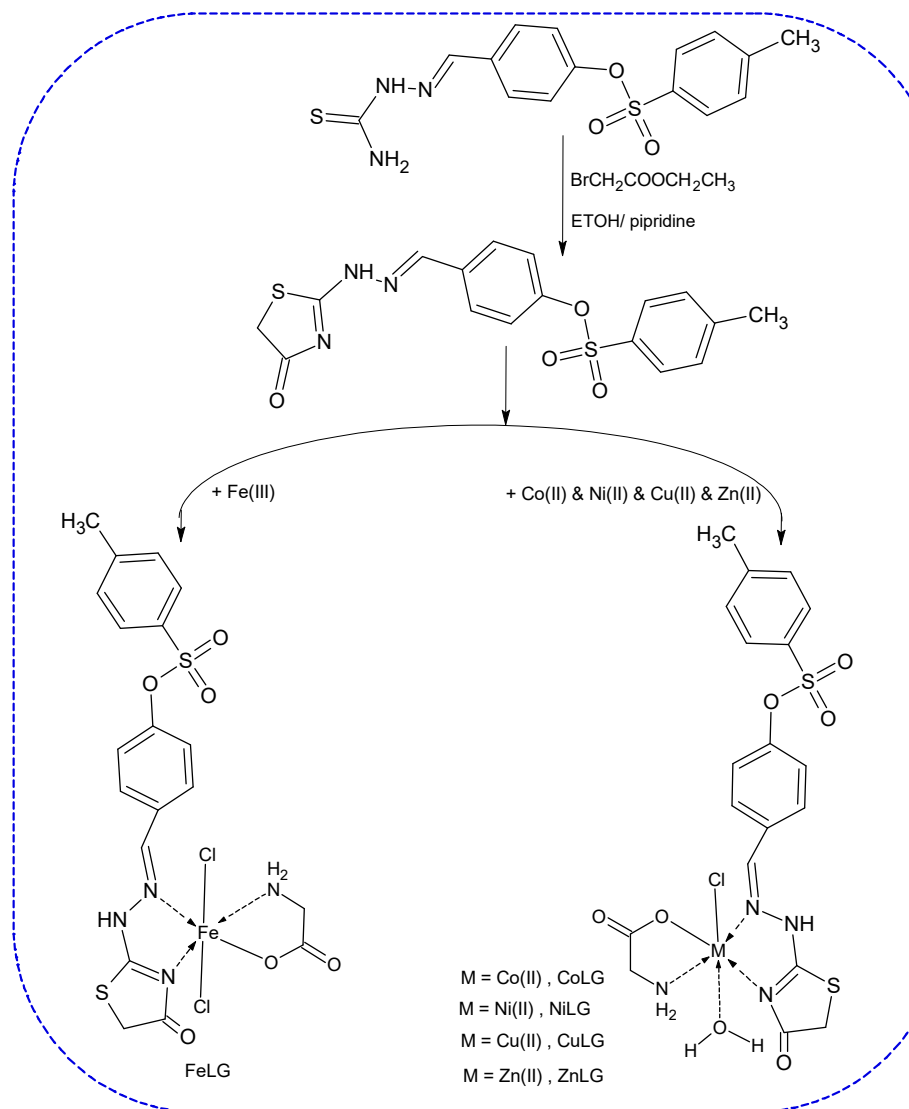
Preparation of the mixed-ligand complexes

The target metal complexes were synthesized according to the previously reported method with slight modification [17, 18]: by mixing 20 mL of the metal salt (0.03 mol) with a mixture of equivalent amounts (0.03 mol) of hot solution ethanol (20 mL) of glycine (HG) and the Schiff-base ligand (L) (M: G: L \equiv 1:1:1 molar ratio). The mix was refluxed in a water bath for 8 hours at 80 °C. The resultant product was filtered and repeatedly cleaned with an H₂O-ethanol solution (1:3). The produced complexes were dried in desiccators over anhydrous calcium chloride, and finally re-crystallized from the water-ethanol mixture (water: ethanol = 1:3).

Characterization

FT-IR spectra were performed using a model 8101 Bruker FTIR in the 4000-400 cm⁻¹ range. The molar magnetic susceptibility of powdered materials was calculated by means of the Bartington (model 4320) susceptibility device. Using a Jenway conductivity meter, the molar conductivities

of 10^{-3} M solutions of the synthesized compounds in DMF were determined. From ambient temperature to 600 °C, the solid complexes underwent TG and DTG thermogravimetric tests. Using a Jenway UV-Vis spectrophotometer, the compounds were subjected to a UV-Vis scan (10^{-3} mol/L acetonitrile solution).



Scheme 1. Preparation of the ligand (L) and corresponding metal complexes.

DFT modeling

For the ligands and metal complexes, respectively, the hybrid correlation functional (B3LYP) [19] in combination with the 6-311 (d, p) [20] and LANL2DZ basis sets [21] were used to optimize

the geometry of the subject compounds [22]. The E_{LUMO} (lowest unoccupied molecular orbitals) and E_{HOMO} (highest occupied molecular orbitals) energies were exploited to estimate quantum chemical strictures: ionization potential (IP), energy gap (ΔE), chemical potential (μ), electronegativity (χ), softness (σ), chemical hardness (η), nucleophilicity index (Nu), electron affinity (EA), maximum electronic charge (ΔN_{max}), and electrophilicity index (ω) [23, 24].

Antimicrobial in vitro testing

The *in vitro* antimicrobial evaluation of the ligands free and their mixed-ligand complexes utilized three fungus strains, two gram-positive and two gram-negative bacteria strains, and two gram-negative bacteria strains. These used strains are *Escherichia coli* (-ve), *Pseudomonas aeruginosa* (-ve), *Staphylococcus aureus* (+ve), *Aspergillus flavus*, *Bacillus cereus* (+ve), *Trichophyton rubrum*, and *Candida albicans*. These strains are frequent pollutants in the Arab environs. Disc diffusion route was used [25].

In the same experimental conditions, the antibacterial and antifungal effectiveness of the compounds under investigation were evaluated in comparison to the conventional antibiotic Clotrimazole [26]. The activity index (AI%) was calculated using the following equation, $\text{AI}\% = (\text{IZ}_t/\text{IZ}_s) \times 100$. IZ_t and IZ_s are rersented the inhibition zone produced by the test compounds and the standard compound, respectively [27].

Molecular docking examination

A computational model of ligand-protein receptor binding was established utilizing the molecular operating environment (MOE). To initiate the process, a high-resolution crystallographic structure of the *E. coli* (pdb ID: 1FJ4) was obtained from the Protein Data Bank [28]. Prior to the docking procedure, a series of meticulous steps were undertaken to prepare the protein, encompassing the removal of solvent molecules and co-ligands, addition of hydrogen atoms, rectification of the protein chain, and identification of active sites [29]. Furthermore, the compounds under investigation underwent optimization for docking through energy minimization, energy adaption, calculation of atomic charges, and assessment of binding energy. Within this domain, a diverse array of structural conformations was scrutinized to evaluate the stability of hydrogen bonds and van der Waals interactions. Subsequently, from a pool of thirty ligand-receptor poses, five conformers that best accommodated the ligand molecule within the protein's active pocket, with the most favorable scoring energy, were selected [30]. The assessment of the ligand and metal complexes' affinity towards the protein was conducted by computing the binding free energy and scrutinizing the hydrogen bonds formed between the ligand and the amino acid residues. This comprehensive computational analysis provided detailed insights into the potential interactions and binding affinities of the compounds with the target protein, offering valuable information for understanding their therapeutic implications.

RESULTS AND DISCUSSION

Structure configuration of the ligand

The prepared ligand was characterized using FT-IR, elemental analysis, $^1\text{H-NMR}$, and $^{13}\text{C-NMR}$ spectra as previously reported by our group [2, 16]. The infrared (IR) spectra of the ligand (L) revealed the disappearance of the $-\text{NH}_2$ group and the emergence of new bands associated with the amidic $-\text{C}=\text{O}$ group at approximately 1725 cm^{-1} . In the $^1\text{H-NMR}$ spectrum obtained in deuterated dimethyl sulfoxide (DMSO-*d*6), various signals were observed, including the exchangeable singlet signals from the $-\text{NH}$ group at δ 11.96 ppm, which disappeared upon deuteration, the $-\text{N}=\text{CH}-$ group at δ 8.38 ppm, the aromatic proton signals ranging from δ 7.77 to

7.12 ppm, and the signals from the active methylene and methyl groups at δ 3.90 and 2.43 ppm, respectively. Furthermore, the ^{13}C -NMR spectra of the molecule indicated the presence of the $>\text{C}=\text{O}$ group at δ 174.53 ppm, as well as signals from the $-\text{CH}_2$ and $-\text{CH}_3$ groups at δ 33.49 and 21.64 ppm, respectively.

Structure configuration of the complexes

Molar conductance and elemental analysis

The produced complexes were soluble in common organic solvents such as acetone, DMF, and DMSO but insoluble in H_2O . The findings of the microanalysis for the metal complexes' carbon, hydrogen, and nitrogen revealed a good covenant between the calculated and discovered values, which supported the suggested formula for the titled metal complexes, Table 1. The values of molar conductivity for prepared complexes were rather low, demonstrating that they were not electrolytes, Table 1.

Binding mode and FTIR spectra

The method of ligand interaction with metal ions was demonstrated using the FTIR spectrum data. By comparing the IR spectra of the metal complexes and those of the free ligands, it was possible to locate the coordination places that might be involved with chelation, Table 1.

Table 1. FTIR of the prepared ligands and corresponding complexes.

		HG	L	FeLG	CoLG	NiLG	CuLG	ZnLG
Elemental analysis Found (calc.) %	C	---	52.43 (52.08)	35.11 (35.42)	37.81 (37.29)	37.08 (37.31)	37.26 (37.01)	35.37 (35.86)
	H	---	3.88 (4.15)	3.28 (3.91)	4.57 (4.12)	4.44 (4.12)	4.30 (4.09)	4.02 (4.28)
	N	---	10.79 (10.18)	8.98 (8.70)	9.07 (9.16)	9.41 (9.16)	9.31 (9.09)	8.51 (8.80)
	M	---	---	8.42 (8.67)	9.39 (9.63)	9.18 (9.60)	10.11 (10.31)	10.14 (10.28)
conductivity	$\mu_{\nu}, \Omega^{-1}\text{cm}^2\text{mol}^{-1}$	---	---	8.98	9.48	10.16	9.95	9.08
IR spectra	ν (-OH)	3326	---	3433	3435	3423	3442	3444
	ν (-NH ₂)	3280	---	3109	3112	3110	3116	3111
	ν (-CH=N)	---	1652	1622	1620	1623	1628	1627
	ν (-COO)asymmetric	1576	---	1591	1588	1598	1584	1588
	ν (-COO)symmetric	1412	---	1419	1420	1423	1422	1418
	ν (C=N) thiazole	---	1597	1522	1527	1525	1530	1528
	ν (M-O)	---	---	538	520	529	535	530
ν (M-N)	---	---	430	434	440	435	440	
UV-vis.	λ_{max}	230	240, 315	434	531	565	590	395
Magnetic	μ_{eff} (B.M)	---	---	5.74	4.42	3.08	1.85	Dia
Stoichiometry	M : L : G	---	---	1:1:1	1:1:1	1:1:1	1:1:1	1:1:1

Strong evidence for the group's (-CH=N) participation in chelation with the metal ion was supplied by the fact that the azomethine group's (1652 cm^{-1}) stretching vibration changed to a lower wavelength range after coordination with the Schiff-base ligand (L), Table 1 [31]. When coordinated, the (C=N) thiazole ring of the pristine ligand at (1597.0 cm^{-1}) was moved to lower wave numbers, providing strong evidence that it participated in chelation with the metal ion.

The $-\text{NH}_2$ group for the glycine co-ligand (HG) was observable at a wavelength of 3280.0 cm^{-1} and migrated to lesser wave numbers upon coordination, as shown in Table 1. This is strong evidence that it took part in the chelation process with the metal ion. The stretching vibrations of $\nu_{\text{sym}}(\text{COO})$ and $\nu_{\text{asym}}(\text{COO})$ were altered to inferior values, indicating cooperation with metal ions [32].

The presence of an extensive peak in the complexes at more than 3400 cm^{-1} has formerly been ascribed to the H_2O molecules' $\nu(-\text{OH})$ groups. The complexes' spectra show new bands in the areas 430-440 and 520-538 that are attributed to $\nu(\text{M-N})$ and $\nu(\text{M-O})$, respectively, Table 1.

Magnetic measurements and electronic spectra

Based on the data presented in Table 1, the UV-Vis spectra of the synthesized compounds indicate a notable bathochromic shift in the typical ligand peak, accompanied by the appearance of distinct peaks in the metal complexes. This observation serves as compelling evidence for the formation of complexes between the metal ions and the ligands. The emergence of new peaks in the spectra suggests a significant alteration in the electronic structure of the compounds upon complexation, signifying the successful coordination of the metal ions with the ligands. One of the best ways to understand the transition metal complexes' structural geometry is to use the effective magnetic moment, $\mu_{\text{eff}} = 2.830 ((Xg * Mwt) - (\text{diamagnetic rectification} * T))^{0.5}$ [33].

Based on the UV-Vis spectra, the FeL complex exhibits bands at 434 nm, which would be consigned to the ${}^6\text{A}_{1g} \rightarrow \text{T}_{2g}(\text{G})$ transitions in the octahedral geometry of the FeL complex. The measured μ_{eff} of FeL complex at room temperature is 5.74 B.M., which would be ascribed to d^5 high spin ($t_{2g}^3 e_g^2$) electron configuration, suggesting an octahedral geometry for the FeL complex, Table 1.

The electronic scale of the CoL complex, revealed a peak at 531 nm, which is assignable to ${}^4\text{T}_{1g}(\text{F}) \rightarrow {}^4\text{T}_{2g}(\text{F})$ conversion, indicating an octahedral geometry. The estimated μ_{eff} of the CoL complex at 25°C is 4.42 B.M., which would be ascribed to d^7 high spin ($t_{2g}^5 e_g^2$) electron configuration, suggesting the CoL complex has an octahedral geometry, Table 1.

The electronic spectrum of the NiL compound, exhibits bands at 565 nm, which may be related to the ${}^3\text{T}_{1g}(\text{F}) \rightarrow {}^3\text{T}_{1g}(\text{P})$ transitions, indicating octahedral geometry around the nickel(II) center, Table 1. The calculated μ_{eff} of NiL compound is 3.08 B.M., back to d^8 ($t_{2g}^6 e_g^2$) electron configuration, suggesting an octahedral geometry, Table 1.

The electronic spectrum of the CuL compound, exhibits bands at 590 nm, which may be associated to the ${}^2\text{B}_{1g} \rightarrow {}^2\text{A}_{1g}$ transitions, indicating octahedral geometry around the copper(II) center, Table 1. The intended μ_{eff} of CuL compound is 1.85 B.M., back to d^9 ($t_{2g}^6 e_g^3$) electron configuration, signifying an octahedral geometry, Table 1.

The electronic spectrum of the ZnL compound, exhibits a band at 395 nm, which might be ascribed to the LMCT ($\text{L} \rightarrow \text{M}$). The diamagnetic character of the ZnL complex would be attributed to the octahedral geometry of the ZnL complex, Table 1.

Stoichiometry of the prepared complexes

The stoichiometry of the prepared metal complexes that were created in solution as a result of the reaction of the metal ion with the researched ligands was established using the molar ratio spectrophotometric technique [34]. Two linear parts of the molar ratio plot's graph overlap at a molar ratio of ≈ 1 which shows how the complex formed in a 1:1:1 ratio (M:L:G).

Thermogravimetric analysis of the synthesized metal complexes

Studying the thermal behavior of metal complex compounds targeted to enhance the complex building's development by calculating the amount of coordinated and uncoordinated H_2O molecules. The prepared complexes exhibited four degradation stages, Table 2. The 1st

degradation stage led to establishing (calc.) a percentage of weight loss of 8.60 (8.39), 7.38 (7.76), 6.37 (5.59), 6.18 (5.59), and 8.93 (8.39) %, indicated the removal of three, two, two, two and two hydrated H₂O molecules for FeLG, CoLG, NiLG, CuLG, and ZnLG, respectively. Whereas, the 2nd degradation stage led to weight-loss calculation of 27.14 (26.71), 15.98 (15.53), 32.88 (33.46), 21.9 (21.12), and 27.84 (27.25) %, suggested the elimination of (C₅H₁₁NOCl₂), (C₅H₁₀NO), (C₈H₁₀N₃O₂Cl), (C₈H₁₀NO), and (C₆H₈N₂O₂Cl) for FeLG, CoLG, NiLG, CuLG and ZnLG, respectively. The thermal decomposition continues for the third and fourth steps leading to the removal of the residual organic moiety leaving the metal oxide as metallic rest, Table 2.

Table 2. Thermal degradation data of the prepared complexes.

Compounds	TG range (°C)	DTG peak (°C)	Mass loss (%)		Assignment	Residue
			found	calculated		
FeLG	30 - 134	97	8.60	8.39	3 H ₂ O	1/2 Fe ₂ O ₃
	134 - 350	290	27.14	26.71	C ₅ H ₁₁ NOCl ₂	
	350 - 520	470	37.19	37.73	C ₁₁ H ₃ N ₂ O ₃ S	
	520 - 610	575	14.17	13.51	C ₃ H ₅ NS	
CoLG	30 - 107	75	7.38	7.76	2 H ₂ O + CH ₂	CoO
	107 - 315	250	15.98	15.53	C ₅ H ₁₀ NO	
	315 - 520	463	48.98	48.68	C ₁₀ H ₄ N ₃ O ₃ ClS ₂	
	520 - 608	576	11.89	11.34	C ₃ H ₅ O ₂	
NiLG	30 - 128	88	6.37	5.59	2 H ₂ O	NiO
	128 - 318	248	32.88	33.46	C ₈ H ₁₀ N ₃ O ₂ Cl	
	318 - 478	398	31.96	31.06	C ₈ H ₁₀ NO ₃ S	
	478 - 599	555	13.98	13.35	C ₃ H ₂ OS	
CuLG	30 - 113	74	6.18	5.59	2 H ₂ O	CuO
	113 - 317	250	21.9	21.12	C ₈ H ₁₀ NO	
	317 - 515	413	41.33	41.85	C ₇ H ₈ NO ₄ ClS ₂	
	515 - 625	595	15.67	14.75	C ₄ H ₃ N ₂ O	
ZnLG	30 - 130	81	8.93	8.39	3 H ₂ O	ZnO
	130 - 332	254	27.84	27.25	C ₆ H ₈ N ₂ O ₂ Cl	
	332 - 482	421	38.88	39.44	C ₁₀ H ₈ NO ₃ S ₂	
	482 - 598	550	11.26	11.02	C ₃ H ₅ NO	

Mass spectra

The suggested molecular formula of the metal complexes [Fe(L)(G)(Cl)]₂.3H₂O, [Ni(L)(G)(H₂O)(Cl)].2H₂O, [Co(L)(G)(H₂O)(Cl)].2H₂O, [Cu(L)(G)(H₂O)(Cl)].2H₂O and [Zn(L)(G)].3H₂O, was established by comparing m/z values with their molecular formula weights. The spectra of FeLG, CoLG, NiLG, CuLG, and ZnLG complexes exhibited the molecular-ion peak (M⁺) at m/z at 643.32, 610.41, 609.43, 615.14, and 636.55 g mol⁻¹, which is worthy covenant the complexes formula weights (644.30, 611.93, 611.69, 616.55, and 636.42). The additional peaks in the spectrum corresponded to different metal complex constituents. It is important to note that the outcomes of the mass spectra correlate well with the C, H, and N findings and the proposed formula.

Interpretation of a complex structure

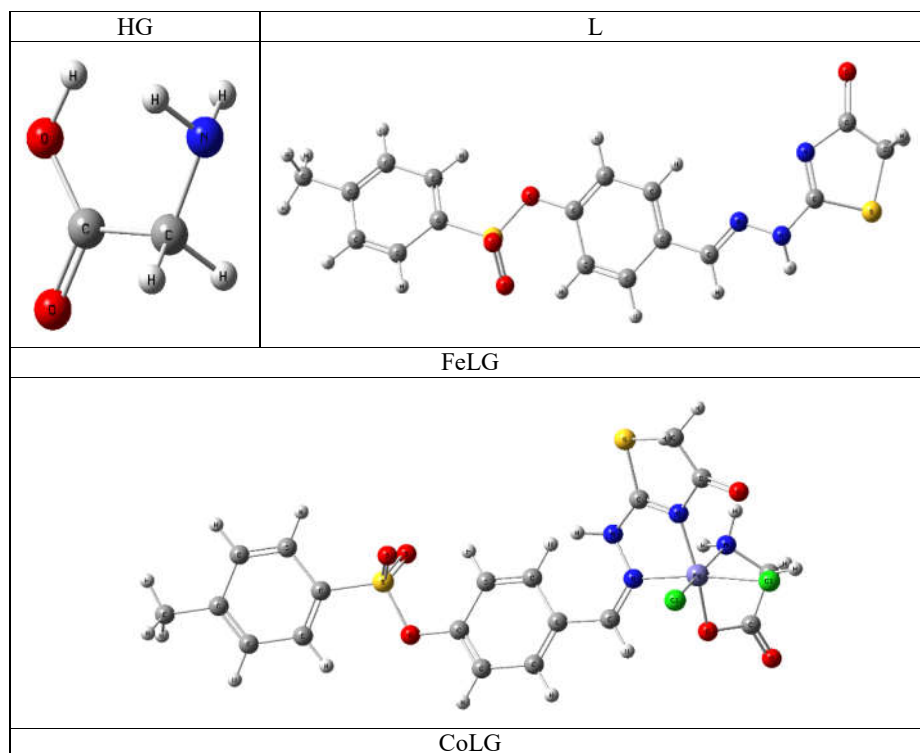
From the correspondence of all the earlier findings, the Schiff ligand (L) participates as a neutral bi-dentate ligand via thiazole Nitrogen and azomethine group, whereas, the co-ligand (HG) glycine participates as a mono-negatively bi-dentate co-ligand thru the carboxylates group, and -NH₂ group, with a metal ion to form M:L:G (1:1:1) as [Fe(L)(G)(Cl)]₂.3H₂O,

[Co(L)(G)(H₂O)(Cl)].2H₂O, [Ni(L)(G)(H₂O)(Cl)].2H₂O, [Cu(L)(G)(H₂O)(Cl)].2H₂O and [Zn(L)(G)].3H₂O for the FeLG, CoLG, NiLG, CuLG and ZnLG, complexes correspondingly, Scheme 1.

DFT modeling

In the lack of X-ray crystal information, molecular modeling is a technology that is becoming increasingly important for the structural analysis of coordination compounds since it provides additional structural details and energy-minimized conformation [35].

Optimization of FeLG, CoLG, NiLG, CuLG and ZnLG complexes provided octahedral geometry around the Fe(III), Co(II), Ni(II), Cu(II), and Zn(II) center, as; [Fe(L)(G)(Cl)₂], [Co(L)(G)(H₂O)(Cl)], [Ni(L)(G)(H₂O)(Cl)], [Cu(L)(G)(H₂O)(Cl)], and [Zn(L)(G)], respectively, Figure 1.



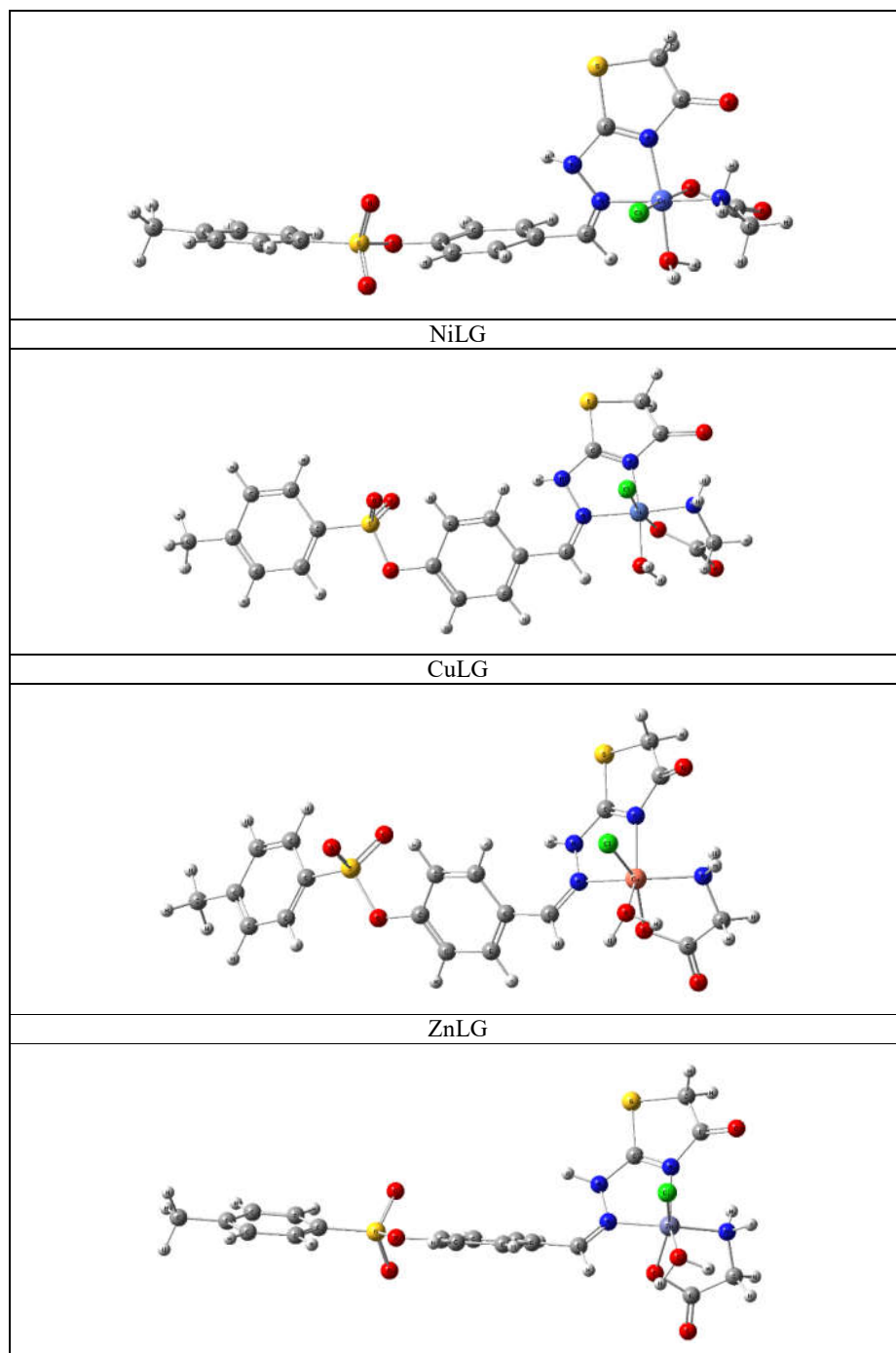


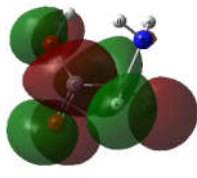
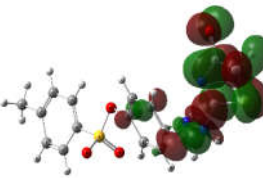
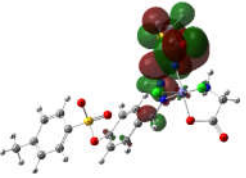
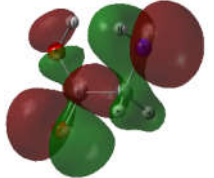
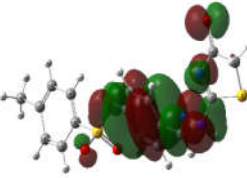
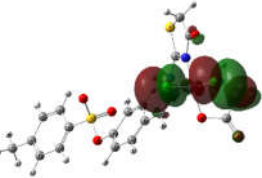
Figure 1. 3D structure of ligand and complexes.

The frontier molecular orbitals (FMOs), HOMO, and LUMO play a significant role in understanding the chemical steadiness, reactivity, optical, and electrical characteristics of a certain molecule (LUMO) [12]. The named complexes' atomic orbital LUMO-HOMO configuration is shown in Fig (2). Consequently, the electrons are predominantly distributed through the molecule. By using HOMO-LUMO energies, ionization potential (IP), energy gap (ΔE), electrophilicity index (ω), electronegativity (χ), chemical potentials (μ), Softness (σ), Chemical hardness (η), nucleophilicity (Nu), and electron affinity (EA) have been intended [36].

HOMO-LUMO energies are recognized as an interesting field in the study of kinetic stability, biological activity, polarizability, chemical reactivity, and softness-hardness of a molecule. The HOMO exemplified the outermost electron-containing orbital and served as an electron contributor. The LUMO substituted for the inmost vacant orbital as an electron acceptor. As a result, a molecule's susceptibility to attack by nucleophiles or electrophiles is determined by its HOMO and LUMO orbitals, respectively [37]. The ΔE , which is the difference between E_{HOMO} and E_{LUMO} , is a sign of the molecules' reactivity. As a result, the smaller ΔE is the molecule that is more responsive to docking. Therefore, the examined compounds' overall reactivity is $\text{ZnLG} > \text{CuLG} > \text{CoLG} > \text{NiLG} > \text{FeLG} > \text{L} > \text{HG}$.

Two more important criteria that affect the chemical reactivity index are softness and hardness. A molecule's inclination to interact with another molecule could be interpreted using the hard-soft-acid-base (HSAB) route; hard acids like to interact with soft acids and hard bases with soft bases. Soft biological species include cells, proteins, and so on. Consequently, soft molecules could interact with biological compounds more readily than hard compounds. Therefore, biological performance rises with rising softness and falls with diminishing values of hardness [38]. Therefore, the order of reactivity has to be $\text{ZnLG} > \text{CuLG} > \text{CoLG} > \text{NiLG} > \text{FeLG} > \text{L} > \text{HG}$.

Consequently, the reactivity sequence can be established as $\text{ZnLG} > \text{CuLG} > \text{CoLG} > \text{NiLG} > \text{FeLG} > \text{L} > \text{HG}$, as indicated by the experimental findings. This order of reactivity reflects the relative tendencies of these metal complexes to undergo specific chemical reactions. The electrophilic activity of these complexes is influenced by their high electrophilicity index value and low chemical potential value [39]. These characteristics contribute to their propensity to engage in electrophilic reactions, thereby influencing their chemical behavior and reactivity in various contexts.

	HG	L	FeLG
LUMO			
	$\uparrow \Delta E$	$\uparrow \Delta E$	$\uparrow \Delta E$
HOMO			
	CoLG	NiLG	CuLG

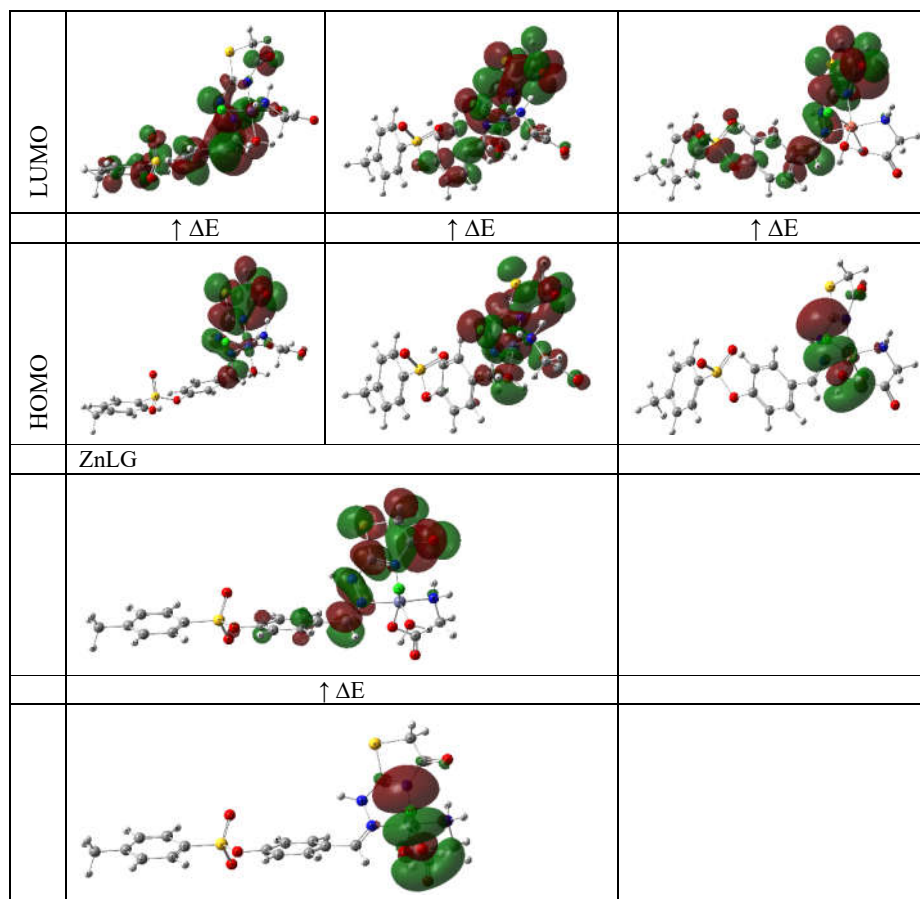


Figure 2. HOMO-LUMO constructions of the investigated ligands and complexes.

Proteins and substrates both contain partial charges, which is a key factor in how quickly a substrate and protein dock [40]. Understanding the 3-dimensional structural and topological characteristics of substrates can be done with the use of the molecular electrostatic potential (MEP) diagram. MEP shows which aspect of molecular geometry—the influence of nuclei or electrons—is prevailing.

Different MEP diagram values are represented by various colors, ranging from blue to red. The negative (red) and positive (blue) parts of the MEP, respectively, are related to nucleophilic and electrophilic reactivity [41]. The red colors exemplify portions of the surface that are negatively charged (i.e., those areas where accepting an electrophile is most promising). The rise in the negative charge of a molecule indicates the interaction of its key sites in interactions with electrophiles.

For the aforementioned compounds, an MEP diagram has been built up at the theoretical level of the optimal shape, Figure 3. Due to their availability of electrons, the glycine oxygen moiety is where the majority of the negative regions (shown red) occur in the substance substrates. These regions are also prime targets for electrophilic assault. The coordinated H₂O moiety, which may

serve as an H-bond donor in protein-substrate intermolecular attractions, is the focus of more positive areas (blue), on the other hand, Figure 3.

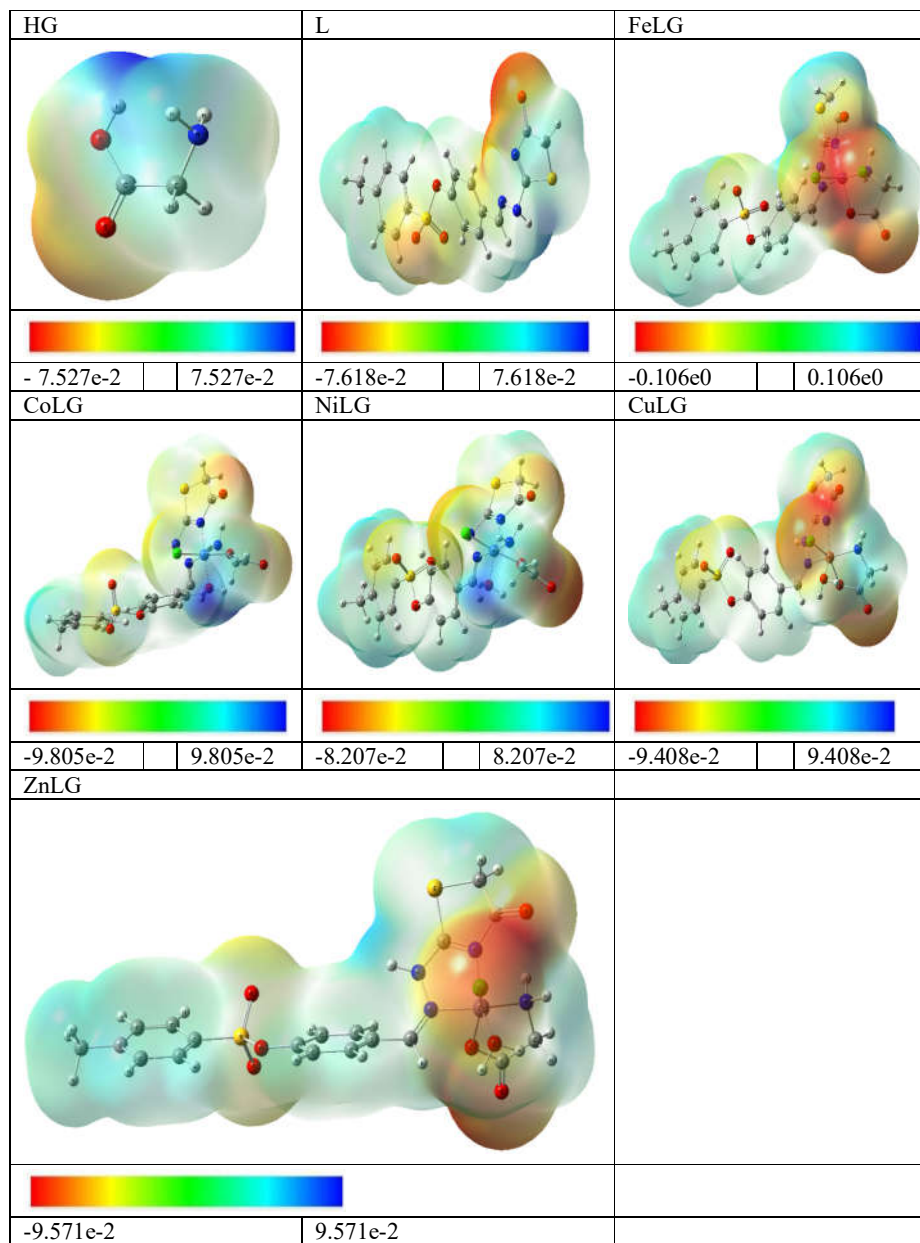


Figure 3. MEP structures of the investigated ligands and complexes.

In vitro antimicrobial screening

In comparison to their free ligands, the novel FeLG, CoLG, NiLG, CuLG, and ZnLG complexes showed greater augmentation in their antibacterial activity with high activity index (%).

FeLG, CoLG, NiLG, CuLG, and ZnLG complexes are more inactive than their pristine ligands, Table (3), could be described according to the chelation concept [42]. According to this theory, chelation diminishes the polarity of the metal ion by partially sharing its positive charge with contributor groups and maybe delocalizing electrons all around the ring. Accordingly, the complex becomes more lipophilic and is therefore more likely to pass through the lipid film of the cell membrane. The complex can obstruct a microorganism's binding centers, disturbing metabolic paths and the cell's respiration process. This prevents protein synthesis, which limits the organism's ability to expand further and leads to the extinction of microorganisms. Additionally, the activity index of the aforementioned compounds varied between 30.00% and 50.00 for free ligands and climbed to be between 60.00% and 94.44% for metal complexes, Table 3.

Table 3. Antimicrobial activity data of the studied ligands and corresponding complexes.

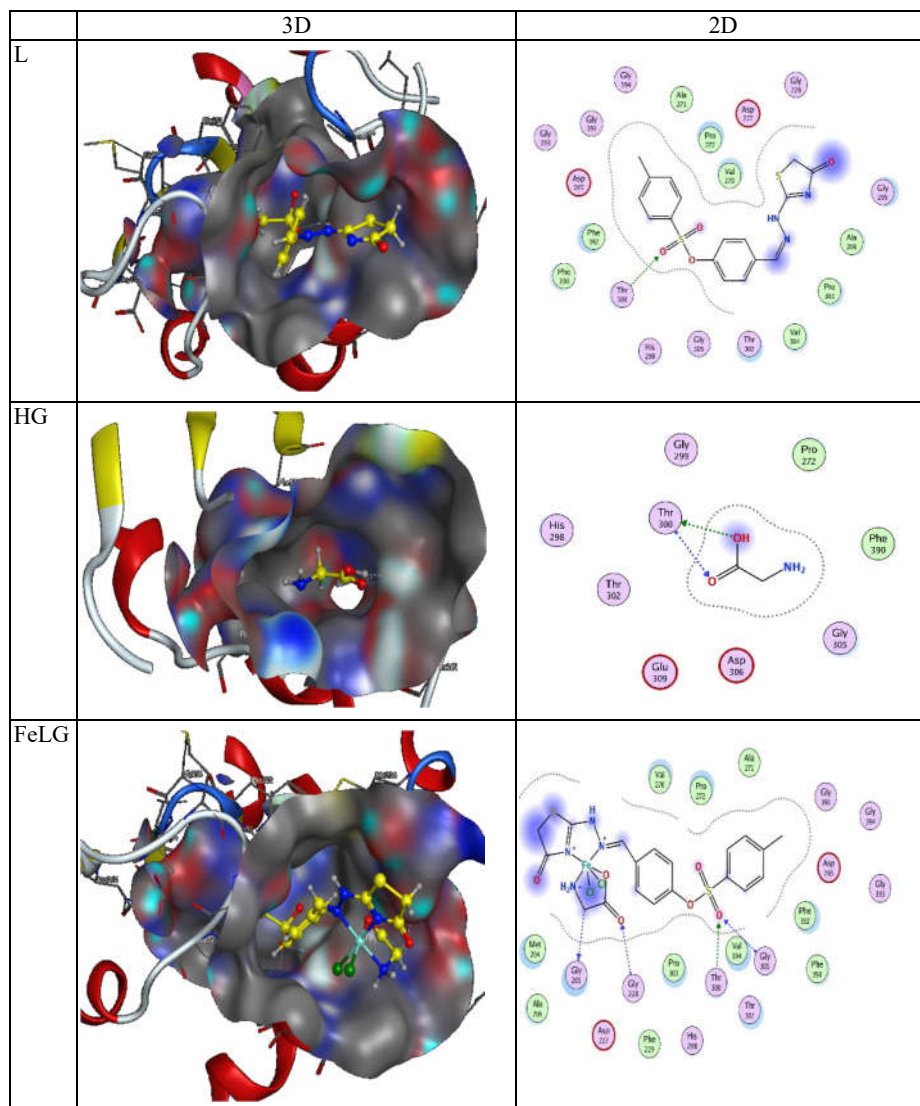
Compounds		HG	L	FeL	CoL	NiL	CuL	ZnL	Clotrimazole
<i>Pseudomonas aeruginosa</i> (-ve)	I _Z , nm	8	9	13	17	15	19	17	21
	%	38.10	42.86	61.90	80.95	71.43	90.48	80.95	
<i>Escherichia coli</i> (-ve)	I _Z , nm	6	8	12	15	12	16	15	20
	%	30.00	40.00	60.00	75.00	60.00	80.00	75.00	
<i>Staphylococcus aureus</i> (+ve)	I _Z , nm	7	9	13	16	13	16	15	19
	%	36.84	47.37	68.42	84.21	68.42	84.21	78.95	
<i>Bacillus cereus</i> (+ve)	I _Z , nm	6	7	14	15	15	16	14	20
	%	30.00	35.00	70.00	75.00	75.00	80.00	70.00	
<i>Aspergillus flavus</i>	I _Z , nm	6	8	15	17	15	17	17	18
	%	33.33	44.44	83.33	94.44	83.33	94.44	94.44	
<i>Trichophyton rubrum</i>	I _Z , nm	7	8	14	16	15	16	15	19
	%	36.84	42.11	73.68	84.21	78.95	84.21	78.95	
<i>Candida albicans</i>	I _Z , nm	7	9	15	16	15	17	16	18
	%	38.89	50.00	83.33	88.89	83.33	94.44	88.89	

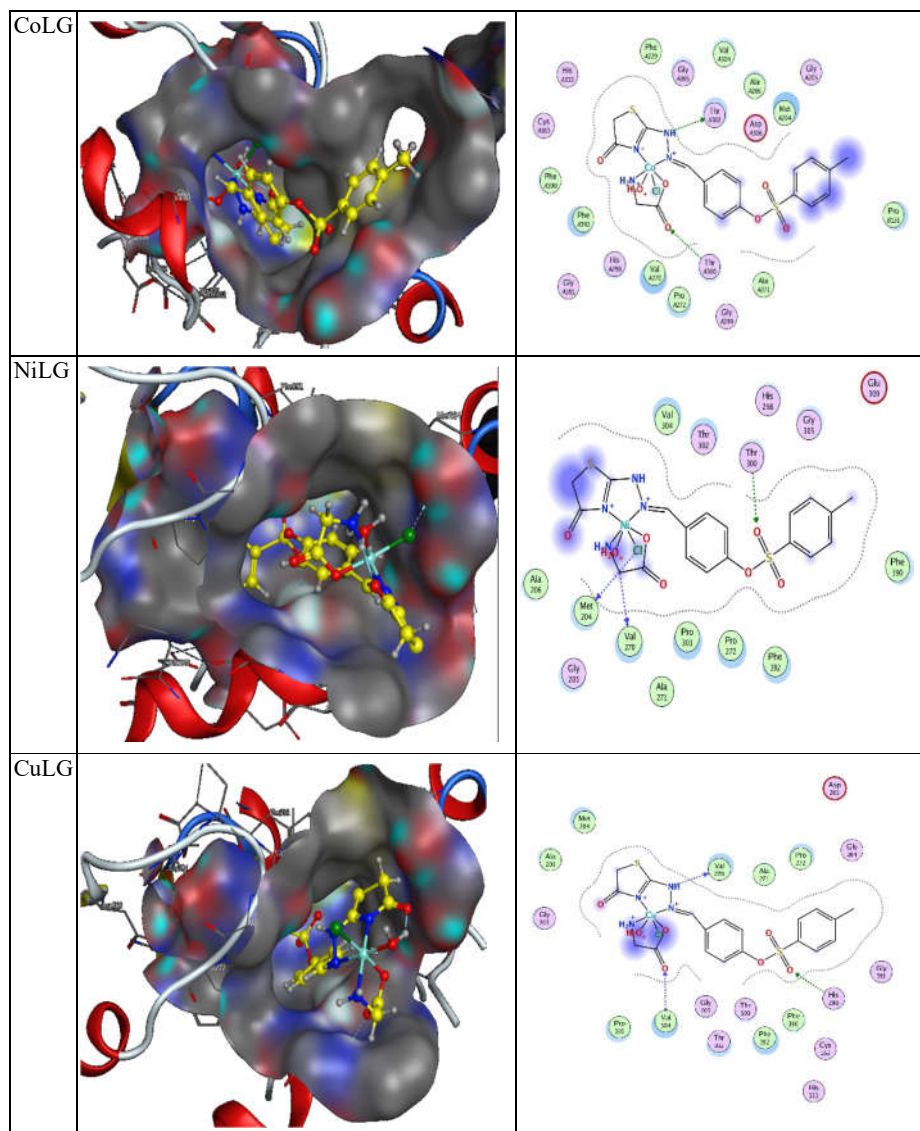
Molecular docking studies

The produced complexes were docked against the antimicrobial target protein in this experiment to determine the relationship between *in vitro* antimicrobial results and inhibitor binding affinities. By rating a compound's composition, molecular docking studies enable virtual compound screening to determine which molecule has the strongest binding affinity [43]. This approach examines how two molecules, such as a substrate and the active site binding of a target receptor, fit together in three dimensions like jigsaw puzzle pieces [44].

In our example, the named chemicals stand in for the substrate, and *E. coli* (PDB ID: 1FJ4) protein is the target receptor [45]. Figure 4 shows the location of the examined substrates' optimal conformation within the binding pocket.

With strong negative docking scores (S), Figure 4 shows the subject substrates bind with the *E. coli* (KAS I, PDB ID: 1FJ4) pocket via a variety of hydrogen bonds and hydrophobic contacts. That shows a robust contact between the active site of the receptor and docked substrates. The inhibitory performance ranked as; ZnLG > CuLG > NiLG > CoLG > FeLG > HL > HG. By incorporating varied hydrogen bond interactions with THR 302, VAL 270, GLY 305, and THR 300, the ZnLG compound, which is the most efficient, was successfully docked to the substrate binding pocket of *E. coli* (KAS I, PDB ID: 1FJ4), as shown in Figure 4.





4. Hasan, H.A.; Mahdi, S.M.; Ali, H.A. Tetradentate azo Schiff base Ni(II), Pd(II) and Pt(II) complexes: Synthesis, spectral properties, antibacterial activity, cytotoxicity and docking studies. *Bull. Chem. Soc. Ethiop.* **2024**, *38*, 99-111.
5. Abu-Dief, A.M.; Said, M.A.; Elhady, O.; Al-Abdulkarim, H.A.; Alzahrani, S.; Eskander, T.N.A.; El-Remaily, M.A.E.A.A.A. Innovation of Fe(III), Ni(II), and Pd(II) complexes derived from benzothiazole imidazolidin-4-ol ligand: Geometrical elucidation, theoretical calculation, and pharmaceutical studies. *Appl. Organomet. Chem.* **2023**, *37*, e7162.
6. Raj, J.; Jain, A.; Sharma, N.; Kumari, A.; Fahmi, N. Synthesis, spectral characterization, and biological activities of novel palladium(II) and platinum(II) complexes of active Schiff base ligands. *Bull. Chem. Soc. Ethiop.* **2023**, *37*, 1383-1396.
7. Ahmed, E.A.; Soliman, A.M.; Ali, A.M.; Ali El-Remaily, M.A.E.A.A.A. Boosting the catalytic performance of zinc linked amino acid complex as an eco-friendly for synthesis of novel pyrimidines in aqueous medium. *Appl. Organomet. Chem.* **2021**, *35*, e6197.
8. Puthilibai, G.; Devatarika, V.; Haewon, B.; Behura, S.S.; Lautre, H.K.; Subha, V.; Sangwan, P.; Sunil, J. Synthesized and hypothesized Schiff base ligand and its metal(II) complexes DNA binding mode. *Bull. Chem. Soc. Ethiop.* **2023**, *37*, 1133-1139.
9. Hamad, H.A.; Nageh, H.; El-Bery, H.M.; Kasry, A.; Carrasco-Marin, F.; Elhady, O.M.; Soliman, A.M.; Ali, M.A.E.A.A.A. Unveiling the exceptional synergism-induced design of Co-Mg-Al layered triple hydroxides (LTHs) for boosting catalytic activity toward the green synthesis of indol-3-yl derivatives under mild conditions. *J. Colloid Interface Sci.* **2021**, *599*, 227-244.
10. Al-Resayes, S.I.; Jarad, A.J.; Al-Zinke, J.M.; Al-Noor, T.H.; El-ajaily, M.M.; Abdalla, M.; Min, K.; Azam, M.; Mohapatra, R.K. Synthesis, characterization, antimicrobial studies, and molecular docking studies of transition metal complexes formed from a benzothiazole-based azo ligand. *Bull. Chem. Soc. Ethiop.* **2023**, *37*, 931-944.
11. Abu-Dief, A.M.; Said, M.A.; Elhady, O.; Alzahrani, S.; Aljohani, F.S.; Eskander, T.N.A.; Ali, M.A.E.A.A.A. Design, structural inspection of some new metal chelates based on benzothiazol-pyrimidin-2-ylidene ligand: Biomedical studies and molecular docking approach. *Inorg. Chem. Commun.* **2023**, *158*, 111587.
12. El-Remaily, M.A.E.A.A.A.; El-Dabea, T.; El-Khatib, R.M.; Abdou, A.; El Hamd, M.A.; Abu-Dief, A.M. Efficiency and development of guanidine chelate catalysts for rapid and green synthesis of 7-amino-4,5-dihydro-tetrazolo [1,5-a] pyrimidine-6-carbonitrile derivatives supported by density functional theory (DFT) studies. *Appl. Organomet. Chem.* **2023**, *37*, e7262.
13. Ramla, M.M.; Omar, M.A.; El-Khamry, A.-M.M.; El-Diwani, H.I. Synthesis and antitumor activity of 1-substituted-2-methyl-5-nitrobenzimidazoles. *Biorg. Med. Chem.* **2006**, *14*, 7324-7332.
14. Iordache, A.M.; Nechita, C.; Podea, P.; Şuvar, N.S.; Mesaros, C.; Voica, C.; Bleiziffer, R.; Culea, M. Comparative amino acid profile and antioxidant activity in sixteen plant extracts from Transylvania, Romania. *Plants* **2023**, *12*, 2183.
15. Abdel-Rahman, L.H.; Basha, M.T.; Al-Farhan, B.S.; Alharbi, W.; Shehata, M.R.; Al Zamil, N.O.; Abou El-ezz, D. Synthesis, characterization, DFT studies of novel Cu(II), Zn(II), VO(II), Cr(III), and La(III) chloro-substituted Schiff base complexes: aspects of its antimicrobial, antioxidant, anti-inflammatory, and photodegradation of methylene blue. *Molecules* **2023**, *28*, 4777.
16. Elkanzi, N.A.A.; Hrichi, H.; Salah, H.; Albqmi, M.; Ali, M.A.; Abdou, A. Synthesis, physicochemical properties, biological, molecular docking and DFT investigation of Fe(III), Co(II), Ni(II), Cu(II) and Zn(II) complexes of the 4-[(5-oxo-4,5-dihydro-1,3-thiazol-2-yl)hydrazono]methyl}phenyl 4-methylbenzenesulfonate Schiff-base ligand. *Polyhedron* **2023**, *230*, 116219.

17. Abd El-Lateef, H.M.; Khalaf, M.M.; Kandeel, M.; Amer, A.A.; Abdelhamid, A.A.; Abdou, A. New mixed-ligand thioether-quinoline complexes of nickel(II), cobalt(II), and copper(II): Synthesis, structural elucidation, density functional theory, antimicrobial activity, and molecular docking exploration. *Appl. Organomet. Chem.* **2023**, *37*, e7134.
18. Abd El-Lateef, H.M.; Khalaf, M.M.; Kandeel, M.; Abdou, A. Synthesis, characterization, DFT, biological and molecular docking of mixed ligand complexes of Ni(II), Co(II), and Cu(II) based on ciprofloxacin and 2-(1H-benzimidazol-2-yl)phenol. *Inorg. Chem. Commun.* **2023**, *155*, 111087.
19. Arafath, M.A.; Adam, F.; Ahamed, M.B.K.; Karim, M.R.; Uddin, M.N.; Yamin, B.M.; Abdou, A. Ni(II), Pd(II) and Pt(II) complexes with SNO-group thiosemicarbazone and DMSO: Synthesis, characterization, DFT, molecular docking and cytotoxicity. *J. Mol. Struct.* **2023**, *1278*, 134887.
20. Shokr, E.K.; Kamel, M.S.; Abdel-Ghany, H.; El- Remaily, M.A.E.A.A.A.; Abdou, A. Synthesis, characterization, and DFT study of linear and non-linear optical properties of some novel thieno[2,3-b]thiophene azo dye derivatives. *Mater. Chem. Phys.* **2022**, *290*, 126646.
21. Hossain, M.S.; Khushy, K.A.; Latif, M.A.; Hossen, M.F.; Asraf, M.A.; Kudrat-E-Zahan, M.; Abdou, A. Co(II), Ni(II), and Cu(II) complexes containing isatin-based Schiff base ligand: Synthesis, physicochemical characterization, DFT calculations, antibacterial activity, and molecular docking analysis. *Russ. J. Gen. Chem.* **2022**, *92*, 2723-2733.
22. Hrichi, H.; Elkanzi, N.A.; Ali, A.M.; Abdou, A. A novel colorimetric chemosensor based on 2-[(carbamothioylhydrazono) methyl] phenyl 4-methylbenzenesulfonate (CHMPMBS) for the detection of Cu(II) in aqueous medium. *Res. Chem. Intermed.* **2023**, *49*, 2257-2276.
23. Latif, M.A.; Ahmed, T.; Hossain, M.S.; Chaki, B.M.; Abdou, A.; Kudrat-E-Zahan, M. Synthesis, spectroscopic characterization, DFT calculations, antibacterial activity, and molecular docking analysis of Ni(II), Zn(II), Sb(III), and U(VI) metal complexes derived from a nitrogen-sulfur Schiff base. *Russ. J. Gen. Chem.* **2023**, *93*, 389-397.
24. Ali, M.A.; Salah, H.; Gad, M.A.; Youssef, M.A.; Elkanzi, N.A. Design, synthesis, and SAR studies of some novel chalcone derivatives for potential insecticidal bioefficacy screening on *Spodoptera frugiperda* (Lepidoptera: Noctuidae). *ACS Omega* **2022**, *7*, 40091-40097.
25. Abd El-Lateef, H.M.; Khalaf, M.M.; Kandeel, M.; Amer, A.A.; Abdelhamid, A.A.; Abdou, A. Designing, characterization, biological, DFT, and molecular docking analysis for new FeAZD, NiAZD, and CuAZD complexes incorporating 1-(2-hydroxyphenylazo)-2-naphthol (H2AZD). *Comput. Biol. Chem.* **2023**, *105*, 107908.
26. Elkanzi, N.A.A.; Ali, A.M.; Hrichi, H.; Abdou, A. New mononuclear Fe(III), Co(II), Ni(II), Cu(II), and Zn(II) complexes incorporating 4-[(2 hydroxyphenyl)imino]methyl}phenyl-4-methylbenzenesulfonate (HL): Synthesis, characterization, theoretical, anti-inflammatory, and molecular docking investigation. *Appl. Organomet. Chem.* **2022**, *36*, e6665.
27. Murugan, T.; Venkatesh, R.; Geetha, K.; Abdou, A. Synthesis, spectral investigation, DFT, antibacterial, antifungal and molecular docking studies of Ni(II), Zn(II), Cd(II) complexes of tetradentate Schiff-base ligand. *Asian J. Chem.* **2023**, *35*, 1509-1517.
28. Alghuwainem, Y.A.; El-Lateef, H.M.A.; Khalaf, M.M.; Amer, A.A.; Abdelhamid, A.A.; Alzharani, A.A.; Alfarsi, A.; Shaaban, S.; Gouda, M.; Abdou, A. Synthesis, DFT, biological and molecular docking analysis of novel manganese(II), iron(III), cobalt(II), nickel(II), and copper(II) chelate complexes ligated by 1-(4-nitrophenylazo)-2-naphthol. *Int. J. Mol. Sci.* **2022**, *23*, 15614.
29. Shaaban, S.; Abdou, A.; Alhamzani, A.G.; Abou-Krishna, M.M.; Al-Qudah, M.A.; Alaasar, M.; Youssef, I.; Yousef, T.A. Synthesis and in silico investigation of organoselenium-clubbed Schiff bases as potential Mpro inhibitors for the SARS-CoV-2 replication. *Life* **2023**, *13*, 912.
30. Shaaban, S.; Al-Faiyz, Y.S.; Alsulaim, G.M.; Alaasar, M.; Amri, N.; Ba-Ghazal, H.; Al-Karmalawy, A.A.; Abdou, A. Synthesis of new organoselenium-based succinilic and

- maleanilic derivatives and in silico studies as possible SARS-CoV-2 main protease inhibitors. *Inorganics* **2023**, 11, 321.
31. Singh, K.; Thakur, R. Synthesis, spectroscopic studies and biological perspectives of transition metal complexes of N/S donor Schiff base. *Eur. Chem. Bull.* **2016**, 5, 193-201.
 32. Al-Gaber, M.A.I.; Abd El-Lateef, H.M.; Khalaf, M.M.; Shaaban, S.; Shawky, M.; Mohamed, G.G.; Abdou, A.; Gouda, M.; Abu-Dief, A.M. Design, synthesis, spectroscopic inspection, DFT and molecular docking study of metal chelates incorporating azo dye ligand for biological evaluation. *Materials* **2023**, 16, 897.
 33. Abd El-Lateef, H.M.; Khalaf, M.M.; Amer, A.A.; Kandeel, M.; Abdelhamid, A.A.; Abdou, A. Synthesis, characterization, antimicrobial, density functional theory, and molecular docking studies of novel Mn(II), Fe(III), and Cr(III) complexes incorporating 4-(2-hydroxyphenyl azo)-1-naphthol (Az). *ACS Omega* **2023**, 8, 25877-25891.
 34. Abd El-Lateef, H.M.; Khalaf, M.M.; El-Taib Heakal, F.; Abdou, A. Fe(III), Ni(II), and Cu(II)-moxifloxacin-tri-substituted imidazole mixed ligand complexes: Synthesis, structural, DFT, biological, and protein-binding analysis. *Inorg. Chem. Commun.* **2023**, 158, 111486.
 35. Abd El-Lateef, H.M.; Khalaf, M.M.; Amer, A.A.; Abdelhamid, A.A.; Abdou, A. Antibacterial, antifungal, anti-inflammatory evaluation, molecular docking, and density functional theory exploration of 2-(1H-benzimidazol-2-yl)guanidine mixed-ligand complexes: Synthesis and characterization. *Appl. Organomet. Chem.* n/a (n/a), e7299.
 36. Mohapatra, R.K.; Mahal, A.; Ansari, A.; Kumar, M.; Guru, J.P.; Sarangi, A.K.; Abdou, A.; Mishra, S.; Aljeldah, M.; AlShehail, B.M.; Alissa, M.; Garout, M.; Alsayyah, A.; Alshehri, A.A.; Saif, A.; Alqahtani, A.; Alshehri, F.A.; Alamri, A.A.; Rabaan, A A. Comparison of the binding energies of approved mpox drugs and phytochemicals through molecular docking, molecular dynamics simulation, and ADMET studies: An in silico approach. *J. Biosaf. Biosecurity.* **2023**, 5, 118-132.
 37. Abdou, A.; Omran, O.A.; Al-Fahemi, J.H.; Jassas, R.S.; Al-Rooqi, M.M.; Hussein, E.M.; Moussa, Z.; Ahmed, S.A. Lower rim thiacalixarenes derivatives incorporating multiple coordinating carbonyl groups: Synthesis, characterization, ion-responsive ability and DFT computational analysis. *J. Mol. Struct.* **2023**, 1293, 136264.
 38. El-Remaily, M.A.E.A.A.A.; Elhady, O.; Abdou, A.; Alhashmialameer, D.; Eskander, T.N.A.; Abu-Dief, A.M. Development of new 2-(Benzothiazol-2-ylimino)-2,3-dihydro-1H-imidazol-4-ol complexes as a robust catalysts for synthesis of thiazole 6-carbonitrile derivatives supported by DFT studies. *J. Mol. Struct.* **2023**, 1292, 136188.
 39. Jarad, A.J.; Dahi, M.A.; Al-Noor, T.H.; El-ajaily, M.M.; Al-Ayash, S.R.; Abdou, A. Synthesis, spectral studies, DFT, biological evaluation, molecular docking and dyeing performance of 1-(4-((2-amino-5-methoxy)diazenyl)phenyl) ethanone complexes with some metallic ions. *J. Mol. Struct.* **2023**, 1287, 135703.
 40. El-Saghier, A.M.; Enaili, S.S.; Kadry, A.M.; Abdou, A.; Gad, M.A. Green synthesis, biological and molecular docking of some novel sulfonamide thiadiazole derivatives as potential insecticidal against *Spodoptera littoralis*. *Sci. Rep.* **2023**, 13, 19142.
 41. Eman, A.A.; Soliman, A.M.M.; Ali, M.A.; El-Remaily, M.A.A. Boosting the catalytic performance of zinc linked amino acid complex as an eco-friendly for synthesis of novel pyrimidines in aqueous medium. *Appl. Organomet. Chem.* **2021**, e6197.
 42. Al-Ayash, S.R.; Al-Noor, T.H.; Abdou, A. Synthesis and characterization of metals complexes with uracil and uracil derivatives (a review). *Russ. J. Gen. Chem.* **2023**, 93, 987-995.
 43. El-Saghier, A.M.; Enaili, S.S.; Abdou, A.; Hamed, A.M.; Kadry, A.M. An operationally simple, one-pot, convenient synthesis, and in vitro anti-inflammatory activity of some new spirotriazolotriazine derivatives. *J. Heterocycl. Chem.* DOI:10.1002/jhet.4752.

44. El-Saghier, A.M.; Abdou, A.; Mohamed, M.A.; Abd El-Lateef, H.M.; Kadry, A.M. Novel 2-acetamido-2-ylidene-4-imidazole derivatives (El-Saghier reaction): Green synthesis, biological assessment, and molecular docking. *ACS Omega* **2023**, *8*, 30519-30531.
45. Najjar, A.M.; Eswayah, A.; Moftah, M.B.; Ruwida Omar M.K.; R.; Bobtaina, E.; Najwa, M.; Elhisadi, T.A.; Tahani, A.; Tawati, S.M.; Khalifa, A.M.M.; Abdou, A.; DowAltome, A.E. Rigidity and flexibility of pyrazole, s-triazole, and v-triazole derivative of chloroquine as potential therapeutic against COVID-19. *J. Med. Chem. Sci.* **2023**, *6*, 2056-2084.